



## Defluoridation of drinking water using a novel sorbent: lanthanum-impregnated green sand

C.M. Vivek Vardhan\*, M. Srimurali

*Department of Civil Engineering, Sri Venkateswara University, Tirupati, Andhra Pradesh 517501, India, Tel. +91 9985963959, +91 9441975981; email: vivekvardhan2@gmail.com (C.M. Vivek Vardhan)*

Received 5 October 2014; Accepted 16 November 2014

### ABSTRACT

A novel adsorbent, lanthanum-impregnated green sand (LIGS), was investigated as an adsorbent for removal of fluoride from water. LIGS was prepared by thermally impregnating lanthanum onto green sand at 950 °C. It exhibited high fluoride removal capabilities than most other conventionally used sorbents. LIGS was characterized using X-ray powder diffraction and scanning electron microscopy techniques to understand its physicochemical properties. Agitated non-flow batch adsorption experiments were conducted for fluoride removal using LIGS as sorbent. Controlling parameters such as equilibrium sorbent dose, kinetics, influence of pH, and competition of anions were investigated. Isothermal data were analyzed using Langmuir, Freundlich, BET, Sips, and Dubinin–Radushkevich isotherm models to know the sorption potential as well as the mechanism involved in sorption. Regeneration experiments were carried out to assess the reusability of sorbent. It was observed that LIGS could efficiently remove fluoride from various initial concentrations to permissible limits. More than 90% of fluoride was found to be removed in 240 min from normally occurring initial fluoride values of 10 mg L<sup>-1</sup>. The sorption was found to follow pseudo-second-order equation model, suggesting chemisorption. Normally occurring pH conditions were found favorable for fluoride sorption. Sips isotherm model was found to fit well and the maximum adsorption capacity of LIGS for fluoride removal was found to be 3.74 (mg g<sup>-1</sup>). Though most ions did not interfere much, competition was evidenced from the anions, nitrates, and bicarbonates for fluoride sorption onto LIGS.

*Keywords:* Fluoride; Water; Sorption; Rare earth; Lanthanum; Green sand; Kinetics

### 1. Introduction

Fluorosis is a burning problem being faced by human beings at various places across the globe, which is caused due to excessive presence of fluoride

in drinking water. The World Health Organization has set a maximum contamination level of 1.5 mg L<sup>-1</sup> of fluoride in drinking water [1]. Presence of fluoride up to 37 mg L<sup>-1</sup> has been reported in several regions of world [2]. Various technologies such as chemical precipitation [3], membrane separation [4], ion exchange [5], adsorption [6], and electro coagulation [7] have

\*Corresponding author.

been tried with varying degrees of success. Chemical precipitation using lime and alum, commonly known as Nalgonda technique [8], is widely adopted. However, huge quantity of sludge generation and residual aluminum in water are major problems related to it. Among various techniques, adsorption is considered to be more adaptable and can be used at household level [9]. Study of literature revealed that various sorbents were tried for removal of fluoride from water which gave various sorption capacities. Lanthanum-impregnated activated alumina gave a maximum adsorption capacity of  $6.7 \text{ mg g}^{-1}$  [10], *Raphanus sativus* peels biomass  $19.82 \text{ mg g}^{-1}$  [11], Lanthanum hydroxide  $242.2 \text{ mg g}^{-1}$  [12], Lanthanum-impregnated chitosan flakes  $1.27 \text{ mg g}^{-1}$  [13], Lanthanum-incorporated chitosan beads  $4.7 \text{ mg g}^{-1}$  [14], metallurgical grade alumina  $12.57 \text{ mg g}^{-1}$  [15], alum-impregnated activated alumina  $40.68 \text{ mg g}^{-1}$  [16], manganese oxide-coated alumina  $2.851 \text{ mg g}^{-1}$  [17], and magnesia-amended activated alumina  $10.12 \text{ mg g}^{-1}$  [18]. Activated alumina, though widely applied, has got certain drawbacks such as suitability at low pH conditions and low rate of sorption. Recently, rare earth elements such as lanthanum, cerium, and yttrium have been tried and used for removal of heavy metals from water [19]. Lanthanum hydroxide was successfully demonstrated for defluoridation by Na and Park [12]. Jagtap et al. have shown that lanthanum-impregnated chitosan flakes can remove fluoride efficiently from water [13]. However, the problem with pure lanthanum in removing fluoride from water is its electrolytic dissolution in water and formation of complexes with fluoride. So, a method of fixing lanthanum onto a substrate has to be devised. Green sand (GS) is a promising sorbent medium for removing pollutants from water. Waste GS was found to remove zinc from water according to Lee et al. [20]. In the present investigation, lanthanum was impregnated thermally onto GS and tried as an adsorbent for fluoride removal. Various sorption experiments such as equilibrium dosage, kinetics, influence of competing ions, and regeneration studies were carried out and their influences were evaluated.

## 2. Materials and methodology

### 2.1. Chemicals

All chemicals used in this study were of analytical reagent grade and were procured from E. Merck Ltd., India. All glassware used were of Pyrex quality and were soaked and washed with nitric acid and distilled water before use. A stock solution of fluoride ( $100 \text{ mg L}^{-1}$ ) was prepared in the laboratory by dissolving

$221.0 \text{ mg}$  of anhydrous sodium fluoride to make up to a liter of distilled water. Required dilutions of fluoride solutions were prepared from the stock solution. Lanthanum carbonate was purchased directly from Indian Rare Earths Ltd, at Aluva, Kerala, India. GS was procured from Hyderabad, Telangana, India. It was crushed and sieved to pass through a 75 micron sieve to get uniform size. Thermo Scientific Evolution 201 UV-Vis Spectrophotometer was used for analyzing the concentration of fluoride.

### 2.2. Adsorbent preparation

About  $0.5 \text{ g}$  of lanthanum carbonate was mixed with  $50 \text{ ml}$  of distilled water, and dilute HCl was added drop wise to it until the lanthanum carbonate dissolved completely. To this,  $20 \text{ g}$  of GS of  $75 \mu\text{m}$  mean size was added. This mixture was mixed for  $3 \text{ h}$  with a magnetic stirrer. The liquid was filtered off and the solids were washed thoroughly with distilled water. It was then dried and heated in a muffle furnace at  $950^\circ\text{C}$  for  $4 \text{ h}$  and cooled. This material is called lanthanum-impregnated green sand (LIGS) and used as adsorbent for all further investigations.

### 2.3. Characterization

X-ray powder diffraction (XRD) studies were carried out on LIGS, before and after adsorption of fluoride to understand its mineralogy. An X-ray diffractometer of Phillips PW-1830 with Cu, K-alpha radiation was used for this purpose. Scanning electron microscope (SEM) of Carl Zeiss EVO MA 15 was used to study the surface morphology of LIGS.

### 2.4. Determination of pH zero point charge ( $\text{pH}_{\text{zpc}}$ )

In brief, six conical flasks each consisting of  $0.01 \text{ M}$  NaCl of  $50 \text{ mL}$  were taken. The pH values of these solutions were adjusted to 2, 4, 6, 8, 10, and 12 using either  $0.1 \text{ N H}_2\text{SO}_4$  or  $0.1 \text{ N NaOH}$ . One gram of LIGS was introduced into each of these flasks and agitated at room temperature for  $48 \text{ h}$  with a shaker. Now pH of each solution was measured and a plot was drawn between initial pH and pH after  $48 \text{ h}$  of agitation. The intersection point of the straight line and curve obtained from points drawn initially and after  $48 \text{ h}$  of agitation gave  $\text{pH}_{\text{zpc}}$ .

### 2.5. Experimental methodology

Appropriately, spiked fluoride solution of  $100 \text{ mL}$  each was taken in  $250 \text{ mL}$  Teflon flasks and measured

quantities of adsorbent were added to it. The flasks were shaken on a rotary shaker of make Kaizen Imperial agitated at 160 rpm. After reaching the equilibrium (240 min), the samples were filtered off using a Whatman size 42 filter paper and analyzed for fluoride concentration. Fluoride was measured using SPANDS method detailed in APHA [21]. The effect of contact time for removal of fluoride was investigated by adding  $6 \text{ g L}^{-1}$  of LIGS into varying concentrations of fluoride. pH studies were carried out by adjusting the solution pH from 3 to 12 using sulfuric acid and sodium hydroxide. Isothermal studies were carried out to know the adsorption capacity of LIGS by varying the initial fluoride concentration from 5 to  $70 \text{ mg L}^{-1}$ . pH measurements were carried out using a pH analyzer of make Hanna.

### 3. Results and discussion

#### 3.1. Characterization

XRD patterns obtained before and after sorption are shown in Figs. 1 and 2, respectively, which were analyzed using the software database provided by joint committee on powder diffraction standards.

In Fig. 1, characteristic peaks corresponding to aluminum and iron were observed at  $2\theta$  values of 26.85, 33.25, 44.65, and 55.25. Also characteristic peaks corresponding to Lanthanum were observed at 36.25, 64.55, and 73.25, indicating the presence of lanthanum on GS. In Fig. 2 characteristic peaks got shifted to  $2\theta$  values of 27.55, 44.65, and 45.65, marking the presence of lanthanum fluoride and thus, confirming adsorptive intake of fluoride onto LIGS.

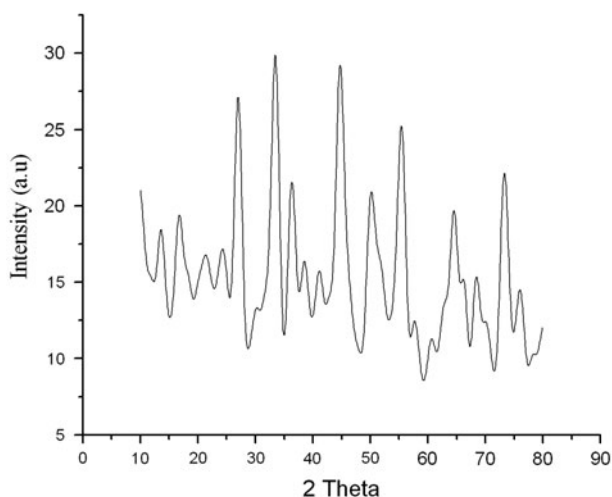


Fig. 1. X-ray diffraction pattern of LIGS before adsorption.

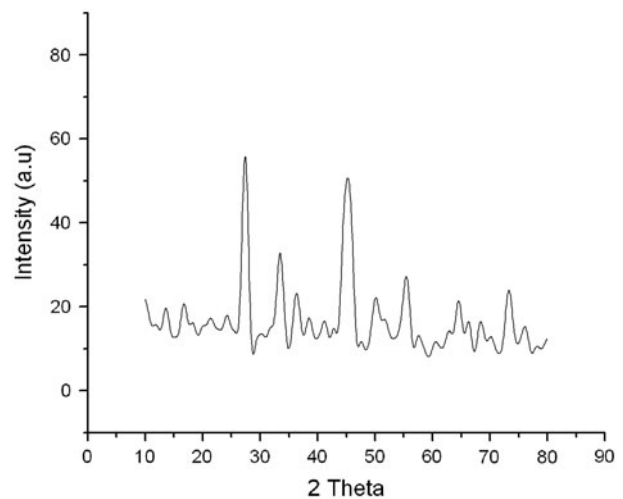


Fig. 2. X-ray diffraction pattern of LIGS after adsorption.

Figs. 3 and 4 show the SEM images of LIGS before and after sorption of fluoride, which clearly indicate the deposition of fluoride.

#### 3.2. Equilibrium adsorbent dose

Knowing the appropriate sorbent dose is crucial in further investigations and also to design a sorption system. Fig. 5 depicts a comparison of influence of doses of LIGS and GS on fluoride removal.

It can be observed that as the dosage of both LIGS and GS were increased gradually, a fluoride removal of 90 and 57%, respectively, took place at  $6 \text{ g L}^{-1}$  for both sorbents. This is less than the value observed by Jagtap et al. [13] who found that lanthanum-impregnated chitosan flakes could remove up to 98% of fluoride from an initial concentration of  $15 \text{ mg F}^{-}/\text{L}$ .

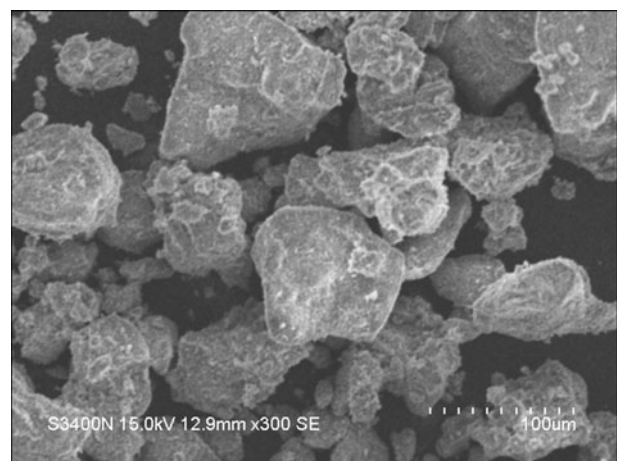


Fig. 3. SEM image of LIGS before adsorption of fluoride.

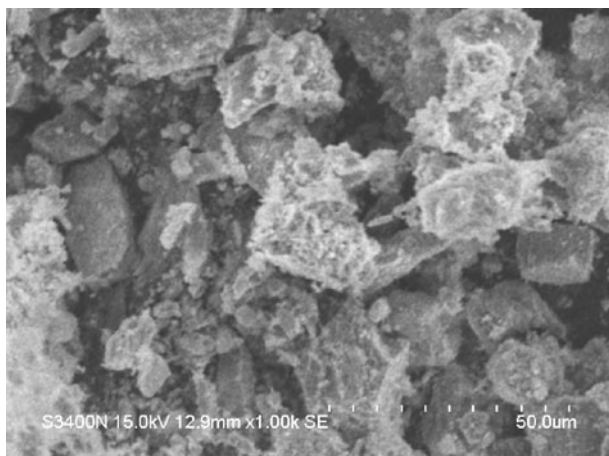


Fig. 4. SEM image of LIGS after adsorption of fluoride.

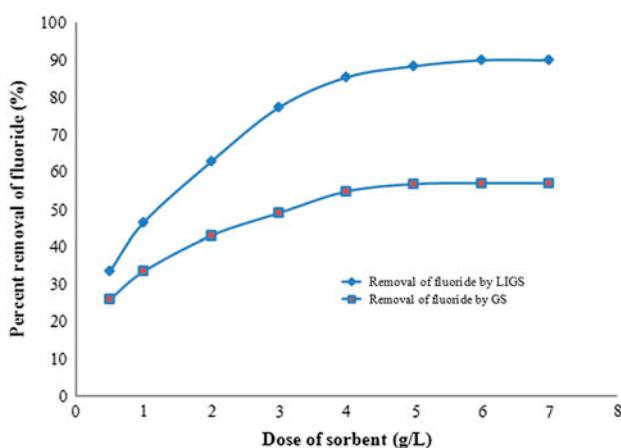


Fig. 5. Comparison of influence of doses of LIGS and GS on fluoride removal.

### 3.3. Influence of pH

pH of solution is a significant parameter that influences fluoride sorption. Fig. 6 shows the influence of pH on defluoridation by both LIGS and GS.

It can be observed from Fig. 6 that fluoride removal was low at low pH values as well as at very high pH values. However, the optimum removal was observed to be at a range of pH 6–9. The mechanism involved, which caused lower rates of adsorption at low pH values, could be formation of weakly charged HF ions, which have a low affinity for the sorbent [22]. HF ions could have formed due to abundant availability of  $H^+$  ions at low pH values. Experimental investigations have shown that  $pH_{zpc}$  of LIGS was 8.7. Also, it was observed that fluoride removal was high between pH 6 and pH 9. This could be due to net

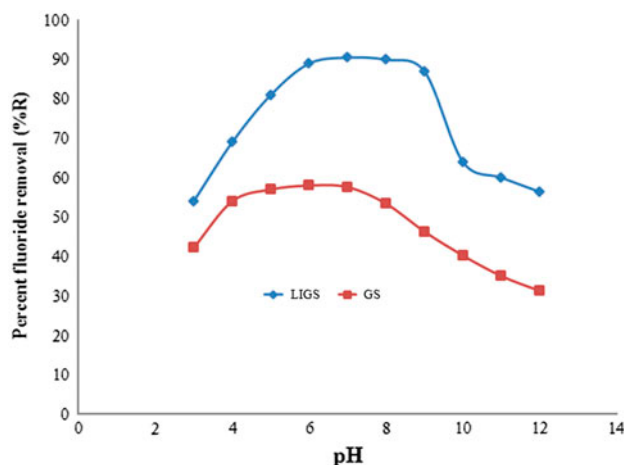


Fig. 6. Influence of pH on defluoridation by LIGS and GS.

positive charge on the sorbent surface up to a  $pH_{zpc}$  value of 8.7 and the less availability of either  $H^+$  ions or  $OH^-$  ions in the range of pH 6–8.7. The concentration of  $OH^-$  ions increases considerably after pH 8.7. This could result in competition of  $OH^-$  ions against  $F^-$  ions for sorption onto the active sorption sites of LIGS. Also, the repulsion of the ions of fluoride by the negatively charged LIGS surface could have resulted in decreased fluoride removal above a pH of 8.9.

### 3.4. Kinetics of fluoride adsorption onto LIGS

Kinetic studies reveal the optimum time for sorption process to reach equilibrium in batch mode. Fig. 7 shows the optimum time required for LIGS at various concentrations of fluoride to reach equilibrium.

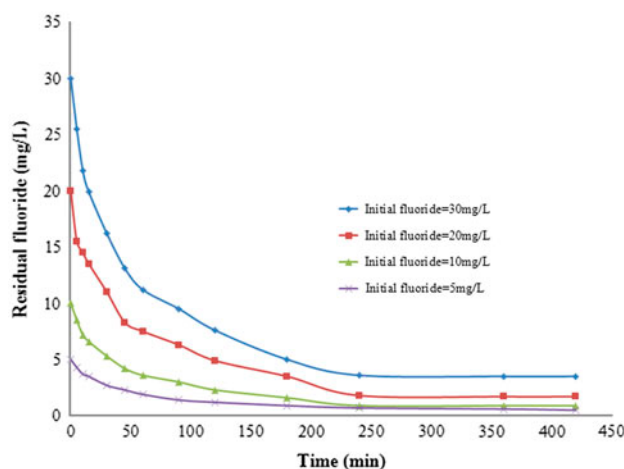


Fig. 7. Kinetics of fluoride removal by LIGS at various initial concentrations of fluoride (adsorbent dose = 6 g  $L^{-1}$ ).

It can be observed that initial fluoride concentration does not influence the time to reach equilibrium, and that the time required to reach the equilibrium was 240 min for all initial concentrations of 5, 10, 20, and 30 mg F<sup>-</sup>/L.

To understand the kinetics of sorption further, the data were fitted into pseudo-first-order, pseudo-second-order, intraparticle diffusion, and Bangham models. According to pseudo-first-order model, the rate of adsorption is proportional to driving force and concentration gradient, whereas according to pseudo-second-order model, the rate of adsorption is proportional to the square of driving force [11].

### 3.4.1. Pseudo-first-order model

The linear form of pseudo-first-order model is given by Eq. (1) [23]

$$\log (q_e - q_t) = \log q_e - \frac{k_1 t}{2.303} \quad (1)$$

where  $q_e$  and  $q_t$  are the amounts of fluoride adsorbed (mg g<sup>-1</sup>) at equilibrium and at time  $t$  (min), respectively, whereas  $k_1$  (L min<sup>-1</sup>) is the adsorption rate constant of first-order adsorption. A plot is drawn between time (min) and  $\log (q_e - q_t)$  and a trend line is drawn to this. Slope of this line gives the value of  $K_1$  (L min<sup>-1</sup>) and its intercept on  $y$ -axis gives the value of  $q_e$  (mg g<sup>-1</sup>). The plot of pseudo-first-order equation is given in Fig. 8. The values of  $K_1$  (L min<sup>-1</sup>) and  $q_e$  (mg g<sup>-1</sup>) found from the plot are given in Table 1.

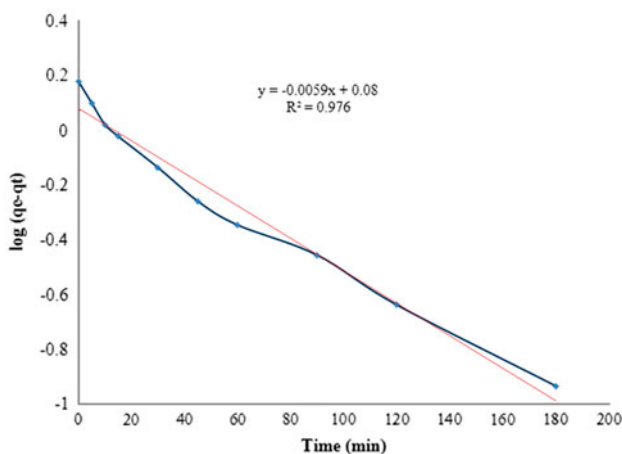


Fig. 8. Plot of pseudo-first-order equation for sorption of fluoride onto LIGS. Adsorbent dose = 6 g L<sup>-1</sup> and Initial fluoride = 10 mg L<sup>-1</sup>.

### 3.4.2. Pseudo-second-order model

The linear form of pseudo-second-order model is given by Eq. (2) [24]

$$\frac{t}{q_t} = \frac{1}{k_2 q_e^2} + \frac{t}{q_e} \quad (2)$$

where  $k_2$  is the rate constant of pseudo-second-order (g(mg min)<sup>-1</sup>). A plot is drawn between time and  $t/q_t$  and a trend line is drawn to it. The equilibrium sorption capacity  $q_e$  (mg g<sup>-1</sup>) is found from the slope of the trend line and the value of  $k_2$  can be found by its intercept value on  $y$ -axis. The plot of pseudo-second-order equation is given in Fig. 9. The calculated (cal) values of  $K_2$  and  $q_e$  are given in Table 1. On a comparison of coefficient of correlation ( $R^2$ ) values of trend lines between pseudo-first-order plot and pseudo-second-order plot, it was observed that the best fit was with pseudo-second-order plot. Furthermore, it was observed that the experimental values of constants were close to calculated values in case of pseudo-second-order model rather than with pseudo-first-order model. This indicates that the type of sorption involved is chemisorption.

Considering that pseudo-second-order model is the best fitting model, further analysis were done to understand the initial sorption rate ( $h$ ) and half adsorption time ( $t_{1/2}$ ) [25] from Eqs. (3) and (4), respectively.

$$h = k_2 q_e^2 \quad (3)$$

$$t_{1/2} = \frac{1}{k_2 q_e} \quad (4)$$

The calculated values of  $h$  (mg g<sup>-1</sup> min<sup>-1</sup>) and  $t_{1/2}$  (min<sup>-1</sup>) are given in Table 1.

### 3.4.3. Intraparticle diffusion model

To find whether intraparticle diffusion is the rate-limiting step, Fick's second law [26] was applied to the experimental data according to Eq. (5).

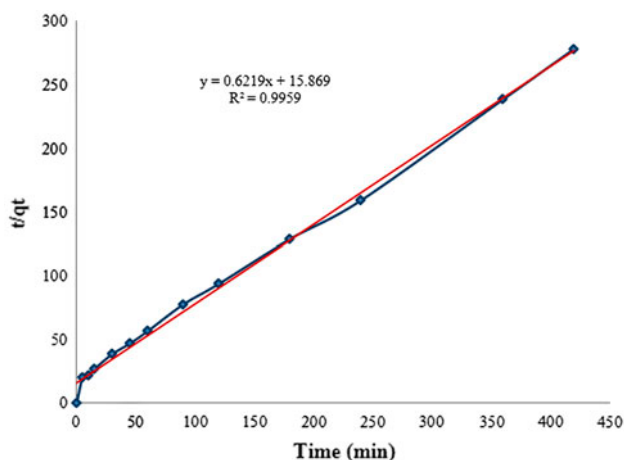
$$q_t = k_{id} t^{1/2} + I \quad (5)$$

where  $k_{id}$  (mg g<sup>-1</sup> min<sup>-1/2</sup>) is the rate constant of intraparticle diffusion and  $I$  is boundary layer effect (mg g<sup>-1</sup>). The value of  $I$  is directly proportional to boundary layer thickness. A plot is drawn between  $q_t$

Table 1

A comparison of parameters of kinetic models for adsorption of fluoride onto LIGS

Pseudo-first-order	Pseudo-second-order	Intraparticle diffusion	Bangham model
$q_e$ (exp) = 1.51 (mg g <sup>-1</sup> )	$q_e$ (cal) = 1.608 (mg g <sup>-1</sup> )	$K_{id}$ = 0.0734 (g mg <sup>-1</sup> min <sup>-1</sup> )	$K_b$ = 0.401
$q_e$ (cal) = 1.202 (mg g <sup>-1</sup> )	$K_2$ = 0.0244 (g mg <sup>-1</sup> min <sup>-1</sup> )	$I$ (cal) = 0.2908 (mg g <sup>-1</sup> )	$\alpha$ = -2.9215
$K$ = 0.0136 (min <sup>-1</sup> )	$h$ = 0.063 (mg g <sup>-1</sup> min <sup>-1</sup> )	$R^2$ = 0.8693	$R^2$ = 0.9422
$R^2$ = 0.976	$t_{1/2}$ = 25.487 (min)		
	$R^2$ = 0.9959		

Fig. 9. Plot of pseudo-second-order equation for sorption of fluoride onto LIGS Adsorbent dose = 6 g L<sup>-1</sup> and Initial fluoride = 10 mg L<sup>-1</sup>.

vs.  $t^{1/2}$ , which gives a straight line whose slope and intercept gives values of  $k_{id}$  and  $I$ , respectively, if the sorption mechanism follows intraparticle diffusion

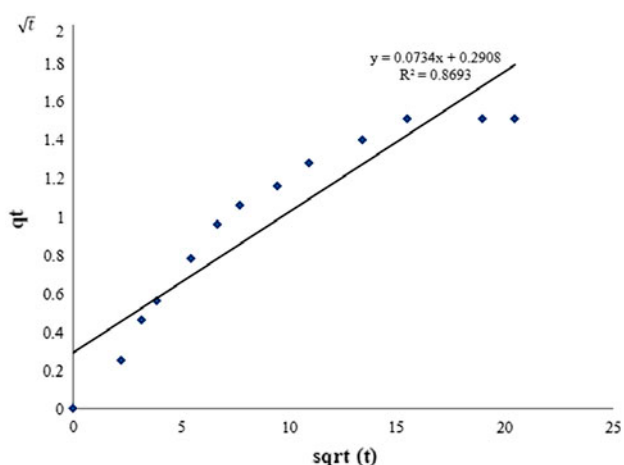


Fig. 10. Intraparticle diffusion plot for sorption of fluoride onto LIGS.

model [27]. The plot of  $q_t$  vs.  $t^{1/2}$  is depicted in Fig. 10 and the values of  $k_{id}$  and  $I$  are given in Table 1. According to Ho [28], the line obtained from plotting  $q_t$  vs.  $t^{1/2}$  should pass through the origin if intraparticle diffusion is the rate-limiting step. However, from Fig. 10, it can be observed that the line has not passed through the origin and so intraparticle diffusion is not the rate-limiting step. This indicates the simultaneous involvement of both boundary layer diffusion and intraparticle diffusion during the adsorption of fluoride onto LIGS.

#### 3.4.4. Bangham's model

Kinetic data were evaluated using Bangham's model [29] to determine the slowest step during adsorption, according to following equation:

$$\log \left[ \log \left( \frac{C_o}{C_o - q_t m} \right) \right] = \log \left( \frac{K_o m}{2.303 V} \right) + \alpha \log(t) \quad (6)$$

where  $C_o$  is the initial concentration of adsorbate in solution (mg L<sup>-1</sup>), while  $V$  is the volume of the solution (L),  $m$  is the weight of adsorbent (g),  $q_t$  (mg g<sup>-1</sup>) is the amount of adsorbate, adsorbed at time  $t$  (min), and  $\alpha$  and  $k_o$  are constants. A graph was plotted between  $\log\{\log[C_o/(C_o - q_t m)]\}$  vs.  $\log(t)$  and is depicted in Fig. 11. If the plot gives a straight line then it indicates that pore diffusion is the rate-controlling step [30]. However, from Fig. 11, it can be observed that the plot yielded a curve which suggests that pore diffusion is not the rate-controlling step. The values of constants  $\alpha$  and  $K_o$  are given in Table 1.

#### 3.5. Adsorption isothermal studies

To understand the adsorption capacity of LIGS for fluoride removal, isothermal data were analyzed using various models. A standard isothermal graph between  $C_e$  and  $q_e$  was plotted for LIGS and GS to understand the nature of sorption. Fig. 12 depicts the standard

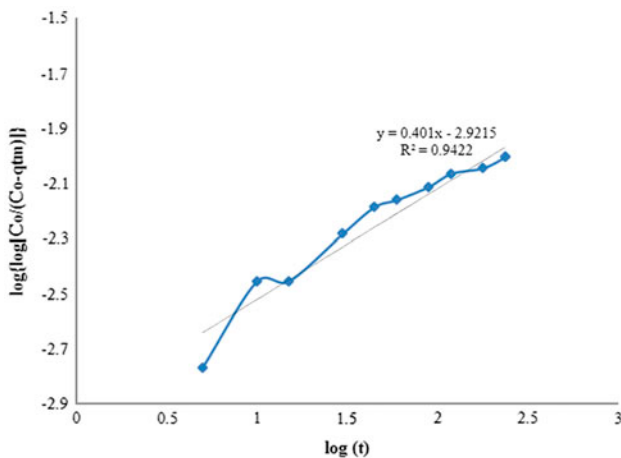


Fig. 11. Plot of bangham model for intra-particle diffusion of fluoride onto LIGS.

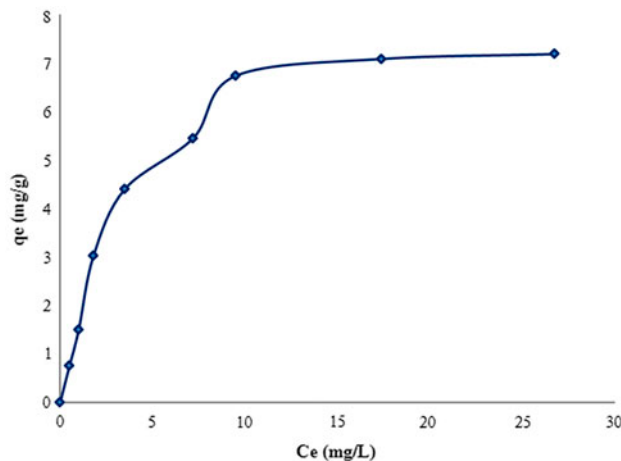


Fig. 12. Standard isotherm plot of sorption of fluoride onto LIGS (fluoride concentration from 5 mg L<sup>-1</sup> to 70 mg L<sup>-1</sup>).

isothermal plot of adsorption of fluoride onto LIGS and Fig. 13 shows the standard isothermal plot of adsorption of fluoride onto GS.

It can be noticed from Fig. 12 that both sorbents are favorable for adsorption. The data were further fit into Langmuir, Freundlich, Sips, BET, and Dubinin–Radushkevich (D–R) models to arrive at the best fitting model.

### 3.5.1. Langmuir isotherm

Langmuir isotherm assumes monolayer sorption over a more or less homogeneous sorbent surface. The linear form of langmuir adsorption isotherm is given by the following Eq. (7) [31].

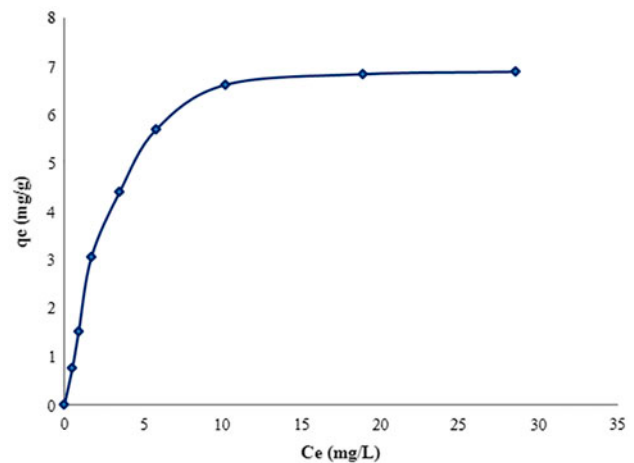


Fig. 13. Standard isotherm plot of sorption of fluoride onto GS (fluoride concentration from 5 mg L<sup>-1</sup> to 70 mg L<sup>-1</sup>).

$$\frac{C_e}{q_e} = \frac{1}{Q_{\max} b} + \frac{C_e}{Q_{\max}} \quad (7)$$

where  $C_e$  (mg L<sup>-1</sup>) is fluoride concentration at equilibrium,  $q_e$  (mg g<sup>-1</sup>) is amount of fluoride adsorbed at equilibrium,  $Q_{\max}$  (mg g<sup>-1</sup>) is maximum adsorption capacity, and  $b$  (L mg<sup>-1</sup>) is a constant related to energy.

### 3.5.2. Freundlich isotherm

Freundlich isotherm model indicates surface heterogeneity of the sorbent surface. The linear form of Freundlich isotherm is given in Eq. (8) [32].

$$\ln q_e = \ln K_f + (1/n) \ln C_e \quad (8)$$

where  $K_f$  is a constant related to adsorption capacity and  $(n)$  is a constant which indicates adsorption intensity.

### 3.5.3. BET isotherm

BET isotherm indicates multiple layers of adsorption. It also assumes that a given layer of sorbent need not complete formation prior to initiation of subsequent layers. The linear form of BET isotherm is given in Eq. (9) [33].

$$C_e / [(C_s - C_e)q_e] = 1/BQ^0 + [(B - 1)/BQ^0](C_e/C_s) \quad (9)$$

Table 2  
Comparison of isothermal constants for adsorption of fluoride onto LIGS

Isotherm model	Langmuir	Freundlich	BET	Sips	D-R
Isotherm parameters	$Q_{\max} = 12.285 \text{ mg g}^{-1}$ $b = 0.971$	$q_e = 1.607 \text{ mg g}^{-1}$ $n = 1.786$	$Q^o = 0.397 \text{ mg g}^{-1}$ $B = 76.32$	$q_{\max} = 3.74 \text{ (mg g}^{-1}\text{)}$ $K_s = 1.7065$	$X_m = 6.437 \text{ (mg g}^{-1}\text{)}$ $K = 0.0056$ $E = 9.432 \text{ kJ mol}^{-1}$
$R^2$	0.9896	0.8983	0.9062	0.9469	0.8961

Table 3  
Comparison of maximum adsorption capacities of various sorbents

Adsorbent	$q_{\max} \text{ (mg g}^{-1}\text{)}$	References
Lanthanum-impregnated activated alumina	6.7	[10]
Raphanus sativus peels biomass	19.82	[11]
Lanthanum hydroxide	242.2	[12]
Lanthanum-impregnated chitosan flakes	1.27	[13]
LIGS	3.74	Present
Lanthanum-incorporated chitosan beads	4.7	[14]
Metallurgical grade alumina	12.57	[15]
Alum-impregnated activated alumina	40.68	[16]
Manganese oxide-coated alumina	2.851	[17]
Magnesia-amended activated alumina	10.12	[18]

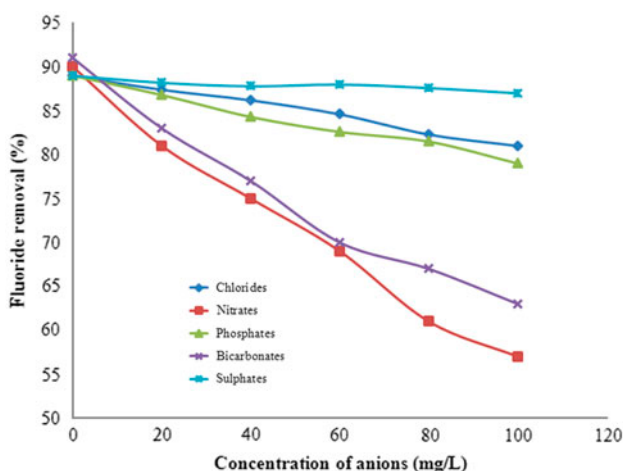


Fig. 14. Influence of competing anions on sorption of fluoride onto LIGS (initial fluoride =  $10 \text{ mg L}^{-1}$  and Sorbent dose =  $6 \text{ g L}^{-1}$ ).

where  $C_s \text{ (mg L}^{-1}\text{)}$  is saturation concentration of solute,  $Q^o$  is number of moles of solute adsorbed per unit weight of adsorbent, and  $B$  is a constant denoting the energy of interaction with the surface.

#### 3.5.4. Sips isotherm

Sips isotherm [34] combines the features of both Freundlich isotherm and Langmuir isotherm. It

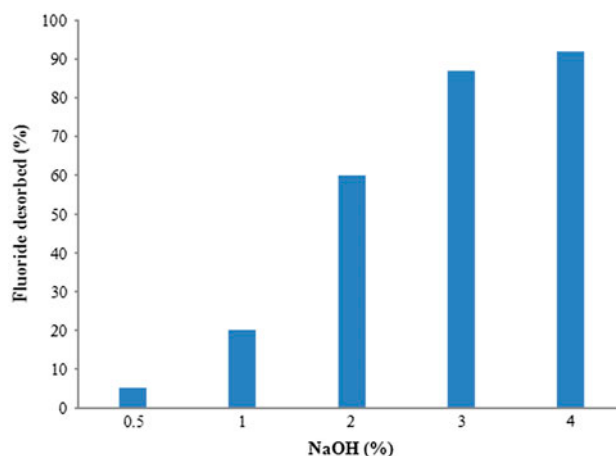


Fig. 15. Fluoride eluted at various concentrations of sodium hydroxide (initial fluoride concentration =  $10 \text{ mg L}^{-1}$ , initial sorbent dose =  $10 \text{ g L}^{-1}$ , and time = 2 h).

effectively overcomes the inherent limitations of both Langmuir and Freundlich isotherms. At low values of  $C_e$ , Sips isotherm acts as Freundlich isotherm, while at high values of  $C_e$ , it exhibits the characteristics of Langmuir isotherm.

The linear form of Sips isotherm is given by following equation:

$$\frac{1}{q_e} = \frac{1}{q_{\max} K_s} \left( \frac{1}{C_e} \right)^{\frac{1}{n}} + \frac{1}{q_{\max}} \quad (10)$$

where  $q_{\max}$  (mg g<sup>-1</sup>) is the maximum sorption capacity of sorbent and  $K_s$  denotes the intensity of sorption.

### 3.5.5. D–R model

Langmuir and Freundlich isotherms give only preliminary information about adsorption mechanism. Therefore, to understand the mechanism involved in adsorption of fluoride onto LIGS, equilibrium sorption data were analyzed using D–R isotherm equation [35].

D–R equation is given by following equation:

$$X = X_m \exp(-K\varepsilon^2) \quad (11)$$

where the Polanyi potential ( $\varepsilon$ ) =  $RT \ln[1 + (1/C)]$ ,  $X$  is the amount of adsorbate adsorbed per unit weight of adsorbent (mg g<sup>-1</sup>),  $X_m$  is the adsorption capacity (mg g<sup>-1</sup>),  $C_e$  is the equilibrium concentration of fluoride in aqueous solution (mg L<sup>-1</sup>), and  $K$  is the constant related to adsorption energy.  $R$  is gas constant and  $T$  is temperature in Kelvins.

The linear form of D–R equation is given by following equation:

$$\ln X = \ln X_m - K\varepsilon^2 \quad (12)$$

The mean free energy of adsorption ( $E$ ) can be defined as the free energy change, when one mole of ion is transferred to the surface of sorbent, from infinity in solution. The value of  $E$  is calculated from Eq. (13)[36].

$$E = (-2K)^{-0.5} \quad (13)$$

The value of  $E$  describes the mechanism of adsorption involved. If the value of  $E$  is <8 kJ mol<sup>-1</sup>, the mechanism involved is physisorption, whereas if the value of  $E$  is from 8 to 16 kJ mol<sup>-1</sup>, it indicates chemisorption. The value of  $E$  in case of adsorption of fluoride onto LIGS was found to be 9.432 kJ mol<sup>-1</sup>, which suggests that the mechanism involved is chemisorption. A chemical reaction which involved conversion of lanthanum to lanthanum fluoride is also evidenced from the peaks of XRD analysis depicted in Figs. 1 and 2, before and after adsorption. The values of adsorption parameters and values of coefficient of correlation ( $R^2$ ) for all the above isothermal models are given in Table 2. A comparison of maximum adsorption capacities of various sorbents with LIGS is given in Table 3.

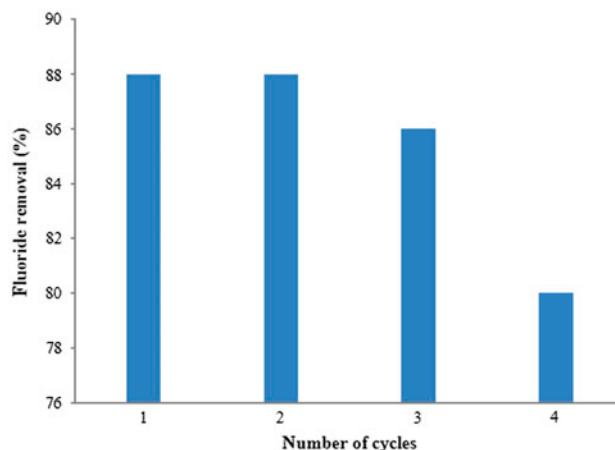


Fig. 16. Removal of fluoride by LIGS after regeneration with sodium Hydroxide (initial fluoride = 10 mg L<sup>-1</sup>, dose of LIGS = 6 g L<sup>-1</sup>, pH = 7, and agitation time = 240 min).

### 3.6. Influence of competing ions

Naturally occurring waters may consist of ions in addition to fluoride ions and they may interfere in the process of fluoride adsorption. To identify their influence, coexisting anions were spiked in addition to fluoride and the effect on adsorption potential of LIGS was observed. Fig. 14 shows the impact of competing coexisting ions on fluoride uptake.

It is clear from the plot that chlorides, sulfates, and phosphates had a negligible impact, whereas bicarbonates and nitrates impeded the sorption process to a considerable extent.

### 3.7. Regeneration studies

Material conservation is essential in any process. To conserve the adsorbent, LIGS, its reusability was examined by treating the loaded sorbent with various eluents. A 4% NaOH solution was found to effectively desorb 92% of adsorbed fluoride from LIGS. The details of various doses of NaOH on the spent sorbent and its potential to desorb fluoride are presented in Fig. 15.

Efficiency of fluoride removal after consecutive cycles of elution by NaOH is presented in Fig. 16.

It can be seen that at the third cycles the sorption efficiency was 86%, whereas at fourth cycle it fell down to 80%.

## 4. Conclusions

In this investigation, a new adsorbent called LIGS was prepared, characterized, and studied for its

fluoride removable capabilities from drinking water. LIGS was able to remove fluoride more efficiently than GS. The main conclusions drawn are as follows:

- (1) pH wielded its influence on fluoride sorption. But the favorable range was found to be between pH 6 and pH 9 for LIGS and pH 5 and 7 for GS, which is a very favorable range for normally occurring conditions of water.
- (2) Fluoride sorption was rapid in the initial 60 min and gradually attained equilibrium at 240 min. Pseudo-second-order equation fitted the data well indicating chemisorption. Mass-transfer curves indicated that the diffusion mechanisms involve both boundary layer diffusion as well as intraparticle diffusion, occurring simultaneously.
- (3) Isothermal studies revealed that Sips isotherm was the best fitting model and the sorption capacity was found to be 3.74 (mg g<sup>-1</sup>).
- (4) Competition of anions for active sites on LIGS was exhibited by bicarbonates and nitrates, whereas chlorides, sulfates, and phosphates did not compete much.
- (5) A 4% sodium hydroxide solution effectively regenerated LIGS by desorbing 92% of adsorbed fluoride. Three cycles of regeneration retained the adsorption capacity of LIGS by maintaining its fluoride removal potential up to 86% from an initial fluoride concentration of 10 mg L<sup>-1</sup>.

## References

- [1] WHO, Guidelines for Drinking-water Quality first Addendum, third ed., vol. 1 recommendations, 2006. Available from: <<http://www.who.int/watersanitationhealth/dwq/gdwq0506.pdf>>.
- [2] Z. Bo, H. Mei, Z. Yongshen, L. Xueyu, Z. Xuelin, D. Jun, Distribution and risk assessment of fluoride in drinking water in the west plain region of Jilin province, China, *Environ. Geochem. Health* 25 (2003) 421–431.
- [3] B.D. Turner, P. Binning, S.L.S. Stipp, Fluoride removal by calcite: Evidence for fluorite precipitation and surface adsorption, *Environ. Sci. Technol.* 39 (2005) 9561–9568.
- [4] K.L. Salipira, R.W. Krause, B.B. Mamba, T.J. Malefetse, L.M. Cele, S.H. Durbach, Cyclodextrin polyurethanes polymerized with multi-walled carbon nanotubes: Synthesis and characterization, *Mater. Chem. Phys.* 111 (2008) 218–224.
- [5] S. Maurice, O.Y. Kojima, O. Aoyi, C. Eileen, B.H. Matsuda, Adsorption equilibrium modeling and solution chemistry dependence of fluoride removal from water by trivalent-cation-exchanged zeolite F-9, *J. Colloid Interface Sci.* 279 (2004) 341–350.
- [6] C.M. Vivek Vardhan, J. Karthikeyan, Removal of fluoride from water using low-cost materials, *Int. Water Technol. J. I* (2) (2011) 1–12.
- [7] R.C. Meenakshi, Maheshwary, Fluoride in drinking water and its removal, *J. Hazard. Mater.* 137 (1) (2006) 456–463.
- [8] K.R. Bulusu, B.B. Sundaresan, B.N. Pathak, W.G. Nawlakhe, D.N. Kulkarni, V.P. Thergaonkar, Fluoride in water, defluoridation methods and their limitations, *J. Inst. Eng. (India), Environmental Engineering Division* 60 (1979) 1–25.
- [9] M. Srimurali, A. Pragathi, J. Karthikeyan, A study on removal of fluorides from drinkingwater by adsorption on to low-cost materials, *Environ. Pollut.* 99 (1998) 285–289.
- [10] J. Chenga, X. Meng, C. Jing, J. Hao, La<sup>3+</sup>-modified activated alumina for fluoride removal from water, *J. Hazard. Mater.* 278 (2014) 343–349.
- [11] M.A. Ashraf, M.A. Rehman, Y. Alias, I. Yusoff, Removal of Cd(II) onto *Raphanus sativus* peels biomass: Equilibrium, kinetics, and thermodynamics, *Desalin. Water Treat.* 51 (2013) 4402–4412, doi: 10.1080/19443994.2012.752333
- [12] C.-K. Na, H.-J. Park, Defluoridation from aqueous solution by lanthanum hydroxide, *J. Hazard. Mater.* 183 (2010) 512–520.
- [13] S. Jagtap, M.K. Yenkie, S. Das, S. Rayalu, Synthesis and characterization of lanthanum impregnated chitosan flakes for fluoride removal in water, *Desalination* 273 (2011) 267–275.
- [14] A. Bansiwali, D. Thakre, N. Labhshetwar, S. Meshram, S. Rayalu, Fluoride removal using lanthanum incorporated chitosan beads, *Colloids Surf., B* 74 (2009) 216–224.
- [15] L. Pietrelli, Fluoride wastewater treatment by adsorption onto metallurgical grade alumina, *Anal. Chim.* 95 (2005) 303–312.
- [16] S.S. Tripathy, J.-L. Bersillon, K. Gopal, Removal of fluoride from drinking water by adsorption onto alum-impregnated activated alumina, *Sep. Purif. Technol.* 50 (2006) 310–317.
- [17] S.M. Maliyekkal, A.K. Sharma, L. Philip, Manganese-oxide-coated alumina: A promising sorbent for defluoridation of water, *Water Res.* 40 (2006) 3497–3506.
- [18] S.M. Maliyekkal, S. Shukla, L. Philip, I.M. Nambi, Enhanced fluoride removal from drinking water by magnesia-amended activated alumina granules, *Chem. Eng. J.* 140 (2008) 183–192.
- [19] A.M. Raichur, M. Jyothi Basu, Adsorption of fluoride onto mixed rare earth oxides, *Sep. Purif. Technol.* 24 (2001) 121–127.
- [20] T. Lee, J.-W. Park, J.-H. Lee, Waste green sands as reactive media for removal of zinc from water, *Chemosphere* 56(6) (2004) 571–581.
- [21] APHA, AWWA, WEF, Standard Methods for the Examination of Water and Wastewater, nineteenth ed., Washington, DC, 1996, p. 657.
- [22] S.S. Tripathy, A.M. Raichur, Abatement of fluoride from water using manganese dioxide-coated activated alumina, *J. Hazard. Mater.* 153 (2008) 1043–1051.
- [23] S. Lagergren, Zur theorie der sogenannten adsorption gelöster stoffe (About the theory of so-called adsorption of soluble substances), *K. Sven. Vetenskapskad. Handl.* 24 (1898) 1–39.

- [24] Y.S. Ho, G. McKay, The kinetics of sorption of divalent metal ions onto sphagnum moss peat, *Water Res.* 34 (2000) 735–742.
- [25] L. You, W. Zhijian, T. Kim, K. Lee, Kinetics and thermodynamics of bromophenol blue adsorption by a mesoporous hybrid gel derived from tetraethoxysilane and bis(trimethoxysilyl) hexane, *Colloid Interface Sci.* 300 (2006) 526–535.
- [26] J. Li, C.J. Werth, Modeling sorption isotherms of volatile organic chemical mixtures in model and natural solids, *Environ. Toxicol. Chem.* 18 (2002) 1377–1383.
- [27] Z. Bekci, C. Özveri, Y. Seki, K. Yurdakoc, Sorption of malachite green on chitosan bead, *J. Hazard. Mater.* 154 (2008) 254–261.
- [28] Y.S. Ho, Removal of copper ions from aqueous solution by tree fern, *Water Res.* 37 (2003) 2323–2330.
- [29] C. Aharoni, S. Sideman, E. Hoffer, Adsorption of phosphate ions by collodion-coated alumina, *J. Chem. Technol. Biotechnol.* 29 (1979) 404–412.
- [30] I.D. Mall, V.C. Sivastava, N.K. Agawal, I.M. Mishra, Removal of congo red from aqueous solution by bagasse fly ash and activated carbon: Kinetic study and equilibrium isotherm analyses, *Chemosphere* 61 (2005) 492–501.
- [31] I. Langmuir, The adsorption of gases on plane surface of glass, mica and platinum, *J. Am. Chem. Soc.* 40 (1916) 1361–1403.
- [32] H.M.F. Freundlich, Über die adsorption in lösungen (About the adsorption in solution), *Z. Phys. Chem.* 57 (1906) 385–470.
- [33] J. Brunauer, P.H. Emmett, E. Teller, Adsorption of gases in multimolecular layers, *J. Am. Chem. Soc.* 60 (1938 and 1940) 309–319.
- [34] R. Sips, Structure of a catalyst surface, *J. Chem. Phys.* 16 (1948) 490–495.
- [35] M.M. Dubinin, L.V. Radushkevich, Equation of the characteristic curve of activated charcoal, *Proc. Acad. Phys. Chem. Sec. U.S.S.R.* 55 (1947) 331–337.
- [36] M. Afzal, S.M. Hasany, H. Ahmad, F. Mahmood, Adsorption studies of cerium on lead dioxide from aqueous solution, *J. Radioanal. Nucl. Chem.* 170(2) (1993) 309–319.